

Special
Collection

Tumor Carbohydrate Associated Antigen Analogs as Potential Binders for Siglec-7

Cristina Di Carluccio^{+, [a]}, Francesco Milanese^{+, [b]}, Monica Civera,^[c] Celeste Abreu,^[d] Sara Sattin,^[c] Oscar Francesconi,^[b] Antonio Molinaro,^[a, e] Ondřej Vaněk,^[d] Roberta Marchetti,^{*, [a]} and Alba Silipo^[a, e]

We investigated two recently synthesized and characterized sialyl derivatives, bearing the Neu5Ac- α -(2-6)-Gal epitope, as promising binders for Siglec-7, an inhibitory Siglec mainly found on natural killer cells. A variety of sialoglycan structures can be recognized by Siglec-7 with implications in the modulation of immune responses. Notably, overexpression of sialylated glycans recognized by Siglec-7 can be associated with the progression of several tumors, including melanoma and renal cell carcinoma. NOE-based NMR techniques, including Saturation Transfer Difference and transferred-NOESY NMR, together with molecular docking and dynamic simulations were combined to shed light on the molecular basis of Siglec-7

recognition of two conformationally constrained Sialyl-Tn antigen analogs. We, therefore, identify the ligands epitope mapping and their conformational features and propose 3D models accurately describing the protein-ligand complexes. We found that the binding site of Siglec-7 can accommodate both synthetic analogs, with the sialic acid mainly involved in the interaction. Moreover, the flexibility of Siglec-7 loops allows a preferred accommodation of the more rigid compound bearing a biphenyl moiety at position 9 of the sialic acid that contributed to the interaction to a large extent. Our findings provided insights for developing potential novel high affinity ligands for Siglec-7 to hinder tumor evasion.

Introduction

Siglecs (sialic acid-binding immunoglobulin-like lectins) are a family of mammalian receptors involved in several biological processes, such as cell-cell communication and immune system modulation.^[1,2,3] Their molecular binding to sialic acid as the terminal portion of glycans or glycoproteins on cell surfaces plays a key role in different regulatory processes of immune responses, making them potential targets for treating human diseases, including autoimmunity and cancer.^[4,5]

Siglec-7 is a CD33-related family member, mainly found on innate lymphoid natural killer (NK) cells but also expressed on blood monocytes and dendritic cells.^[6,7] The structure of Siglec-7 is composed of an N-terminal V-set IgG domain that allows the recognition of sialylated glycans, two extracellular C2 domains, and one immunoreceptor tyrosine inhibitory motif (ITIM) in the cytoplasmic tail, which confers the inhibitory function to this protein.^[8] Indeed, the engagement by Siglec-7 of cognate ligands induces the phosphorylation of the ITIM site, which trigger the signaling cascade and, consequently, dampens NK activation and cytotoxicity, maintaining the immune homeostasis in physiological conditions.^[5]

Reduced expression of Siglec-7 on NK cells can be associated with certain types of cancers,^[9] while overexpression of sialylated glycans on cancer cells recruits Siglec-7/9,^[10] inhibiting NK cell activation and leading to tumor development.^[11,12,13] Therefore, it is not surprising that Siglec-7 has been considered an attractive potential therapeutic target to modulate the immune system and overcome tumor progression.^[14]

Depending on the biological context, Siglec-7 can recognize different sialoglycans, including monosialylated structures, such

[a] Dr. C. Di Carluccio,⁺ Prof. A. Molinaro, Prof. R. Marchetti, Prof. A. Silipo
Department of Chemical Sciences
University of Naples Federico II
Via Cintia 4, 80126, Napoli (Italy)
E-mail: roberta.marchetti@unina.it

[b] Dr. F. Milanese,⁺ Prof. O. Francesconi
Department of Chemistry "Ugo Schiff"
University of Florence,
Polo Scientifico e Tecnologico
50019, Sesto Fiorentino, Firenze (Italy)

[c] Dr. M. Civera, Prof. S. Sattin
Dipartimento di Chimica
Università degli Studi di Milano
Via C. Golgi, 19, 20133, Milano (Italy)

[d] C. Abreu, Dr. O. Vaněk
Department of Biochemistry
Faculty of Science
Charles University
Hlavova 2030/8
12800, Prague (Czech Republic)

[e] Prof. A. Molinaro, Prof. A. Silipo
Department of Chemistry
School of Science, Osaka University
Osaka University Machikaneyama
Toyonaka, Osaka, 560-0043 (Japan)

[⁺] These authors contributed equally to this work.

Supporting information for this article is available on the WWW under <https://doi.org/10.1002/ejoc.202300644>

Part of the "DCO-SCI Prize and Medal Winners 2022" Special Collection.

© 2023 The Authors. European Journal of Organic Chemistry published by Wiley-VCH GmbH. This is an open access article under the terms of the Creative Commons Attribution License, which permits use, distribution and reproduction in any medium, provided the original work is properly cited.

as 2,6-linked sialylated structures that contain Neu5Ac- α -(2-6)-Gal, a specific epitope recognized by Siglec-2.^[15,16] Moreover, Siglec-7 can bind glycans containing two sialic acid units linked by a α -2,8 glycosidic linkage, as found in GD3 or GT1b gangliosides.^[17] This may be explained by the alkaline nature of the protein binding site that could favor more negative charges of the two sialic acids.^[18] Interestingly, it has been shown that the flexibility of Siglec-7 allows a conformational change of the CC' loop upon binding.^[19]

We previously evaluated the interactions of human CD22 (h-CD22) with two synthetic analogs of the disaccharide STn,^[20] a tumor carbohydrate associated antigen (TACA). These two compounds (Figure S1) shared a common structure composed of Neu5Ac- α -(2-6)-Gal linked to a lactam ring that mimics the Thr residue found on natural STn antigens but lacking the acetyl group at C2 of the galactose unit. Both synthesized STn analogs showed higher affinity for h-CD22 with respect to the natural ligand, due to rigidity given by the aglycon moiety. Interestingly, the presence of a biphenyl moiety at position 9 of the Neu5Ac contributes to the interaction with h-CD22 but impedes the canonical accommodation of the ligand into the binding site.^[20]

Given the appealing inhibitory activity exhibited by structurally constrained STn derivatives,^[21,22] we decided to prove the ability of the previously synthesized sialyl-TnThr analogs to act as binders also for Siglec-7. Thus, here we describe the molecular recognition of two STn derivatives by Siglec-7, providing information regarding the binding affinities and the ligands' accommodation into the Siglec-7 binding site. Moreover, these studies can be a starting point for the design and synthesis of high-affinity ligands of therapeutic relevance, that may prevent cancer cells from evading the immune system.^[23,24,25]

Results and Discussion

The syntheses of the STn derivatives, analogs 1 and 2, were previously described.^[26,27] The binding analyses between Siglec-7 and analogs 1 and 2 were achieved by a combination of Saturation Transfer Difference (STD) and transferred NOESY (tr-NOESY) NMR experiments together with computational approaches, including docking and molecular dynamic (MD) simulations.^[28,29,30]

Molecular binding of analog 1 to Siglec-7

STD NMR experiments proved the recognition of analog 1 by Siglec-7 (Figure 1). As inferred by comparing the STD and the reference (off-resonance) NMR spectra, changes in the relative intensities and multiplicities of certain proton signals of analog 1 indicated a selective protein-ligand interaction. Undoubtedly, most of the STD signals in the spectrum were attributed to the Neu5Ac, meaning that this residue was recognized by Siglec-7. Almost all protons' signals belonging to the galactose did not give STD response; only its anomeric proton (B1, resonating at a

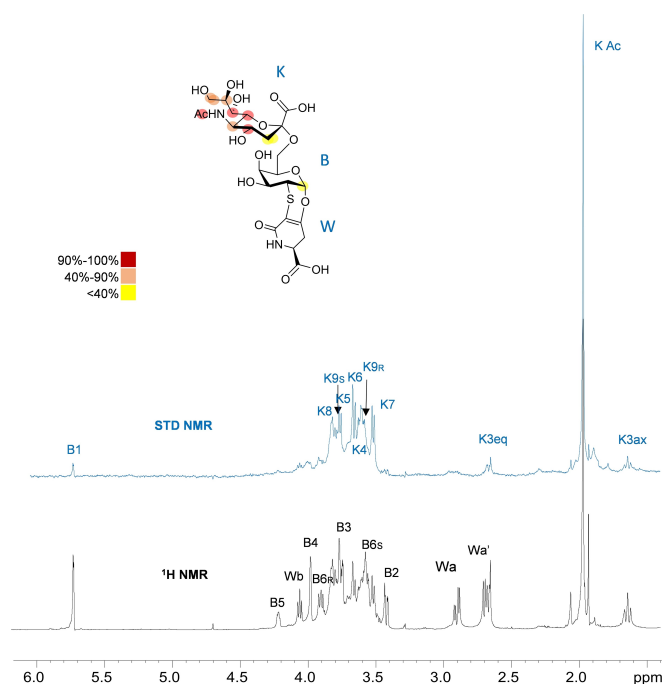


Figure 1. STD NMR analysis of Siglec-7 with analog 1. STD-NMR spectrum (blue) of Siglec-7/analog 1 and the unsaturated reference spectrum (black) allowed to obtain the ligand epitope mapping, calculated by $(I_0 - I_{\text{sat}})/I_0$, where $(I_0 - I_{\text{sat}})$ is the intensity of the signal in the STD-NMR spectrum and I_0 is the peak intensity of the unsaturated reference spectrum (off-resonance). The highest STD intensity was set to 100%, and the %STD of the other protons were normalized to this value.

chemical shift of 5.7 ppm) was observed at a very low intensity. No STD NMR effects were observed for the protons of the lactam ring (indicated as Wa, Wa' and Wb in Figure 1), thus suggesting that this region was completely excluded from the recognition by Siglec-7. Once set the highest STD signal at 100%, the %STD of all the other protons were obtained accordingly. The resulting epitope map of the analog 1 (Figure 1) showed that the acetyl group (ACK) and the proton at position 7 (K7) of Neu5Ac were strongly recognized by Siglec-7, as well as the protons at positions 4 and 6 (K4 and K6). The glycerol chain of Neu5Ac also received a good magnetization from the protein, while the diastereoisotopic protons at position 3 (axial and equatorial, K3A and K3E) gave lower STD effects, like the anomeric proton of the galactose residue (B1).

Regarding the conformational behavior, Neu5Ac α 2-6-Gal glycosidic linkage is generally characterized by three torsion angles, defined by φ (C1-C2-O-C6'), ψ (C2'-O2'-C6-C5) and ω (O6-C6'-C5'-O5').^[31] Previous studies and energy maps demonstrated that φ could populate torsion angles of approximately -60° and 180° , while ψ assumed a value around 180° .^[31,32] On the other hand, ω gives additional flexibility to the linkage, adopting three different values in the free state, corresponding to $180^\circ/60^\circ/-60^\circ$ (tg/gt/gg rotamers). In analog 1, φ torsion angle around Neu5Ac- α -(2-6)-Gal glycosidic linkage for approximately -60° could be deduced, as suggested by the absence of NOE contacts between H6 of galactose and H3 (axial and equatorial protons) of Neu5Ac (Figure S2), that instead would

have been observed if ϕ was 180° .^[20] Computational studies provided further information about the interaction between Siglec-7 and analog **1** and the combination of the NMR experiments permitted to obtain a 3D model (Figure 2).

Docking calculations (GLIDE SP, version 8.0)^[33] unveiled the best poses of analog **1** into the binding site of Siglec-7. The crystal structure of Siglec-7 in complex with a GT1b analog (PDB: 2HRL)^[19] was used as structural template. In the X-ray complex, the terminal sialic acid was the major determinant of ligand binding and as it formed a salt bridge between the sialic acid carboxylate and the guanidinium group of Arg-124. Hydrogen bonds between Asn-133 backbone and the glycol chain were also observed and the acetyl group formed a water-mediated interaction with the backbone NH of Lys133. In agreement with the NMR conformational analysis, Neu5Ac- α -(2-6)-Gal glycosidic linkage ϕ and ψ torsion angles were fixed at the experimental values of -60° and -180° , respectively, while ω torsion angle was free to rotate. In the resulting docking poses, the Neu5Ac moiety formed the X-ray complex key interactions thus confirming its primary involvement in the binding to Siglec-7. In the most representative and energetically favored pose, the carboxylate group of the lactam ring interacted with the side chain of Trp74, a residue of the C–C' loop, forming a hydrogen bond (Figure S3).

This docking pose was selected for an unconstrained MD simulation (Desmond,^[34] 500 ns, NVT conditions, SPC water model^[35]) to assess the stability of the ligand-protein interactions and to allow protein flexibility. During the simulation, the ligand binding to Siglec-7 was stable. The canonical salt bridge between Arg124 and the carboxylate group of Neu5Ac

was stable over the simulation time, together with other polar interactions. Among these, the H-bond occurring between the NH of the acetyl group of Neu5Ac and the Lys131 backbone was observed in the 63% of the sampled structures. The glycerol chain of Neu5Ac was also found permanently in contact with the side chain of Asn133 (96% populated). On the other hand, the galactose and the aglycon did not show interactions with Siglec-7, suggesting they are solvent exposed and the initial hydrogen bond between the lactam and Trp74 was broken. Indeed, during the simulation the ω torsion values settled around 60° (Figure S4), thus leading to a different preferred orientation of the lactam moiety. These data, fully in accordance with the STD NMR results (Figure 1), revealed that the interaction between Siglec-7 and the analog **1** was allowed thanks to the anchorage of the sialic acid, while the rest of the molecule did not influence the binding.

Molecular binding of analog **2** to Siglec-7

STD NMR experiments proved the recognition of analog **2** by Siglec-7 (Figure 3). In particular, the STD enhancements of **2** in the presence of the protein indicated a selective protein-ligand interaction and permitted ligand epitope mapping (Figure 3). Again, most of the protons belonging to the Neu5Ac gave high STD NMR effects. The strongest STD magnetization was transferred from Siglec-7 to the protons at position 4, 7 and those belonging to the acetyl group of sialic acid. High STD effects were also observed for the protons of the biphenyl moiety (chemical shift range of 7.4–7.9 ppm) suggesting a relevant

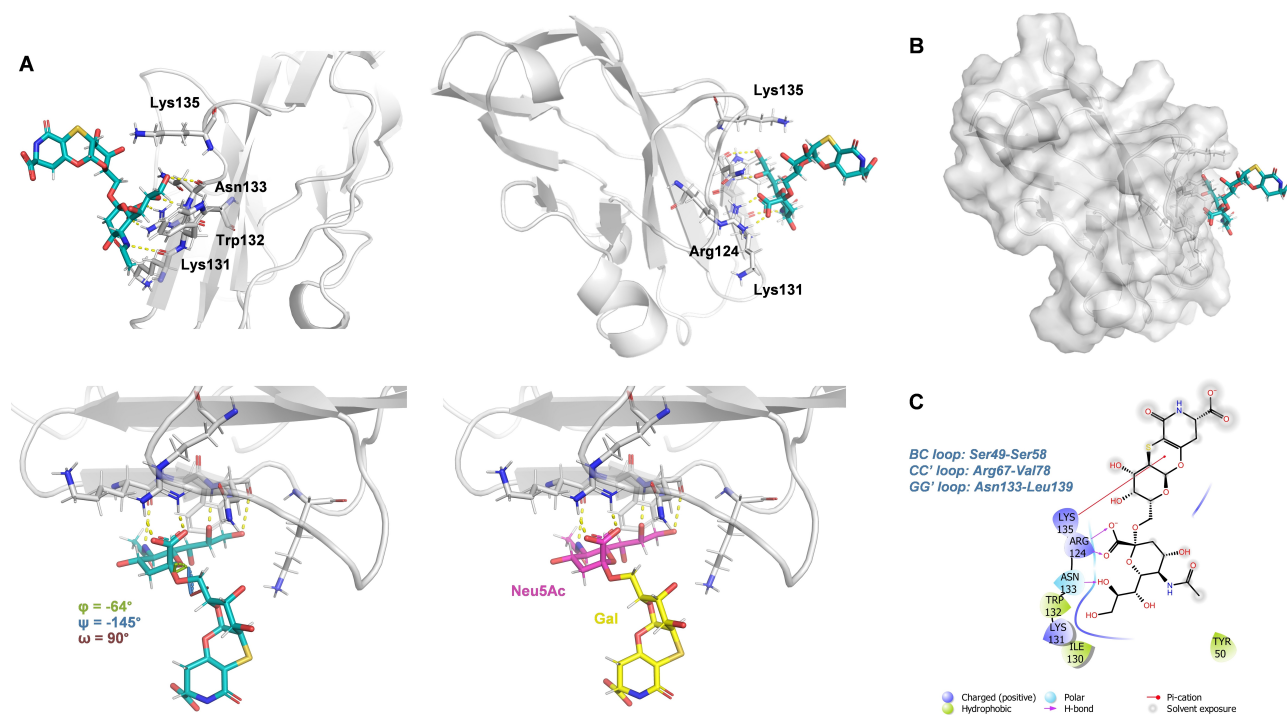


Figure 2. A 3D snapshot of Siglec-7 and analog **1** taken from MD simulations. A) Different 3D views of the complex, with the amino acids of the binding site highlighted. B) 3D complex with protein surface. C) 2D diagram of interactions. The sialic acid was recognized by the protein, while the galactose and ring moiety were solvent exposed.

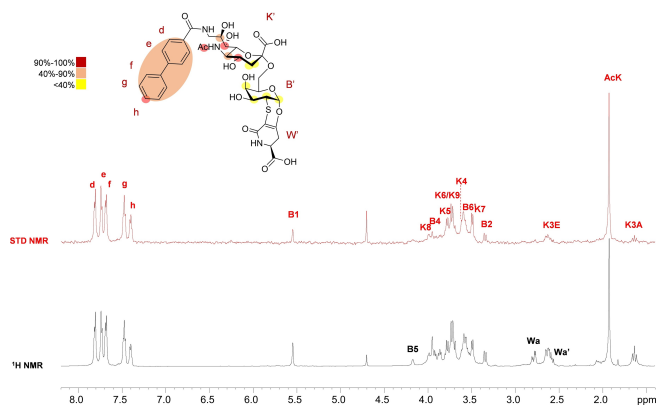


Figure 3. STD NMR analysis of Siglec-7 with analog 2. STD-NMR spectrum (red) of Siglec-7/analog 2 and the unsaturated reference spectrum (black) allowed to obtain the ligand epitope mapping, calculated by $(I_{\text{off}} - I_{\text{sat}})/I_{\text{off}}$, where $(I_{\text{off}} - I_{\text{sat}})$ is the intensity of the signal in the STD-NMR spectrum and I_{off} is the peak intensity of the unsaturated reference spectrum (off-resonance). The highest STD intensity was set to 100%, and the %STD of the other protons were normalized to this value.

contribution to the interaction with Siglec-7. Some protons of the galactose residue also gave STD responses, albeit to a lesser extent, as observed for the isolated protons at positions 1 and 2 (chemical shift values at 5.5 and 3.3 ppm, respectively); the aglycon ring did not give STD response, indicating it did not contribute to the interaction.

Tr-NOESY NMR experiments (Figure S5) of analog 2 interacting with Siglec-7 determined the conformational preferences of the ligand, that assumed a similar conformation around

Neu5Ac- α -(2-6)-Gal glycosidic linkage observed for analog 1 (see above).

A similar computational workflow (docking calculation followed by MD simulation) was applied to characterize the binding of analog 2. In the docking poses, the ligands maintained the sialic acid moiety bound to Arg124 with the ϕ torsion values at around -60° . The lactam group was differently engaged by the protein residues depending on the ω torsion values; the top-ranked pose with a ω torsion angle of 60° was selected for MD (Figure S4) simulation. The docking binding mode was stable during the simulation and the 3D model of Siglec-7 with analog 2, in agreement with NMR data, was proposed (Figure 4).

As observed for 1, a canonical accommodation for the sialic acid of analog 2, with Arg124 making a salt bridge with the carboxylate group of Neu5Ac residue, was observed. Similar to the interaction between Siglec-7 and analog 1, H-bonds involving the Lys131 backbone and the NH of the acetyl group of Neu5Ac (70% populated), as well as the side chain of Asn133 with the glycerol portion of the same sugar residue (96% populated), were found. Furthermore, the biphenyl moiety, that received a strong magnetization from the protein, as observed in the STD NMR spectrum (Figure 3), was involved in cation- π and π - π interactions with Lys135 and Phe122 (38% and 46% populated, respectively). Differently from analog 1, where the galactose unit was completely solvent exposed, in analog 2, this residue was found closer to the binding site making hydrophobic contacts with the side chain of Trp74 (48% populated). In accordance with the absence of STD signals, no markable contacts were found with the aglycone moiety (Figure 3). The

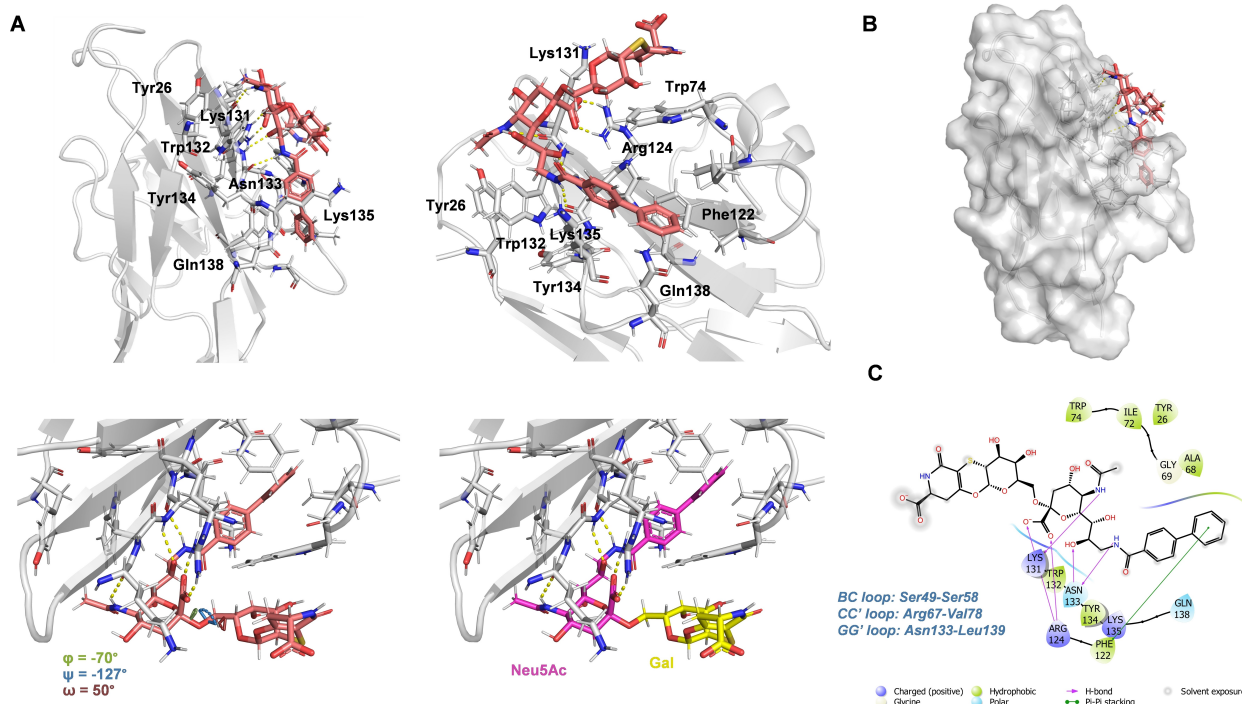


Figure 4. 3D snapshot of Siglec-7 and analog 2 taken from MD simulations. A) Different 3D views of the complex, with the amino acids of the binding site highlighted. B) 3D complex with protein surface. C) 2D diagram of interactions. The Neu5Ac as well as the biphenyl moiety were strongly recognized by the protein, while the aglycone ring was more solvent exposed.

input conformation was conserved among the simulation (Figure S4), thus indicating that both ligands shared a similar preferred bound geometry.

Calculation of the binding affinities of Siglec-7 for analogs 1 and 2

To calculate the binding affinity between Siglec-7 and analog 1, a single-ligand titration NMR experiment was performed.^[36] STD NMR experiments were acquired after consecutive additions of analog 1 to the final concentration of 0.3, 0.4, 0.5, 0.8, 1.1, 1.25 and 2.5 mM in the solution. The STD AF proton values were

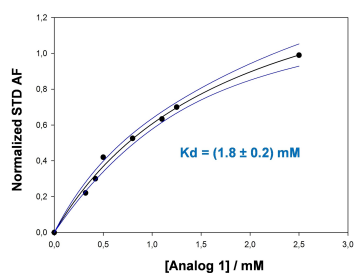


Figure 5. Estimation of the binding affinity calculated by STD NMR; a titration of Siglec-7 with increasing concentrations of analog 1 was performed. A 95% confidence interval (blue bands) was considered for the monoexponentially curve.

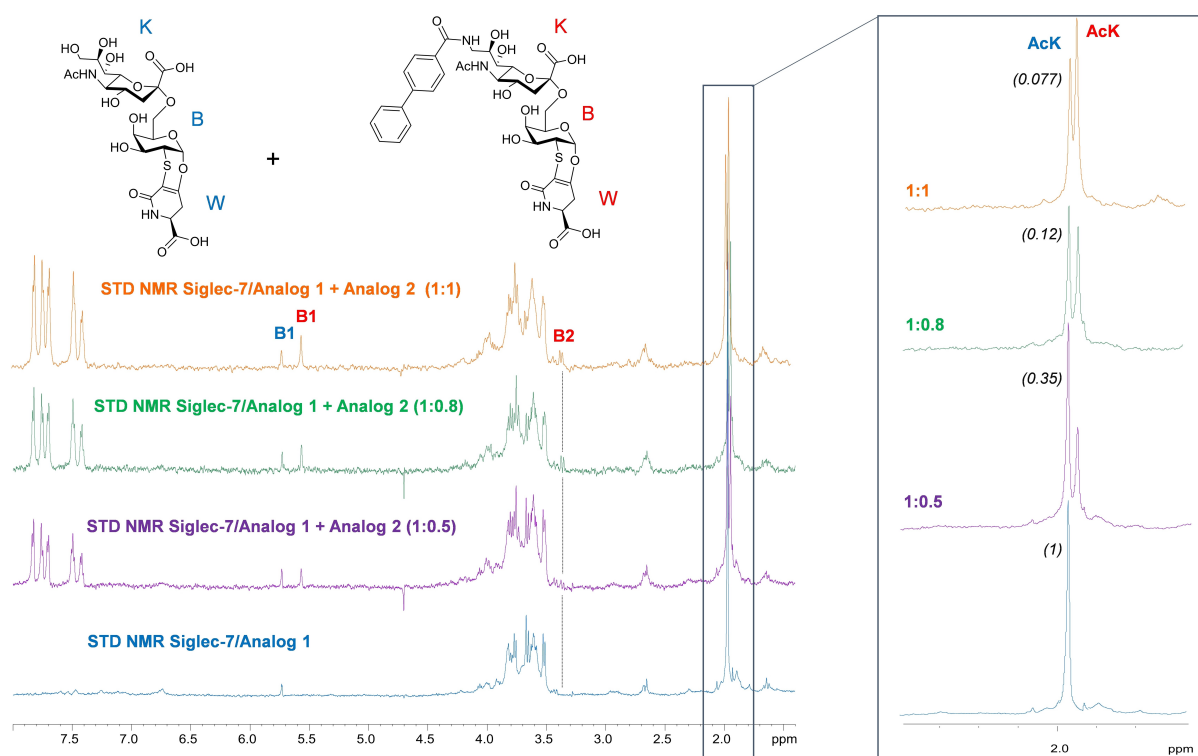


Figure 6. Competition STD NMR experiments allowed to calculate the K_d value of the Siglec-7/analog 2 complex. A mixture of Siglec-7 and analog 1 was titrated with different concentrations of analog 2 (ligands ratios of 1:0, 1:0.5, 1:0.8, 1:1). At a sub-stoichiometric concentration of analog 2 with respect to analog 1, STD NMR signals coming from the competitor were shown. A zoom of the NHAc region was also evidenced. The decrease of STD intensity of analog 1 at increasing concentration of analog 2 (indicated in parenthesis) has been calculated considering the STD NMR spectrum of Siglec-7/analog 1 mixture as reference.

calculated and normalized with respect to the highest value of ligand concentration. A binding isotherm was considered by fitting the STD AF values at different concentrations of analog 1, giving the dissociation constant of 1.8 mM (Figure 5).

Since in analog 2 an additional contribution to the interaction with respect to sialic acid was observed from the biphenyl moiety, NMR competition experiments were performed to determine if analog 2 could compete with analog 1 (Figures 6 and S6).^[37]

The results confirmed that the Siglec-7 binding site involved in the interactions was the same for both analogs. Interestingly, taking advantage of the K_d between Siglec-7 and analog 1 calculated by STD NMR titration experiments (see above, Figure 6), it was further possible to obtain the K_d value for the interaction between Siglec-7 and analog 2. STD NMR experiments were acquired following the progressive addition of the competitor to the mixture of Siglec-7 and analog 1. Then, STD effects were evaluated; as expected, the calculated K_d value of the competitor (analog 2) was 0.33 mM, lower than the K_d of 1, confirming the preference of the Siglec-7 for the sialyl-derivative containing the biphenyl moiety.

These results were in agreement with the binding scores obtained from MD simulations. To estimate the binding free energy of ligands, MM/GBSA calculations were indeed performed, confirming the higher affinity of analog 2 ($-81.39 + / - 7.69$ kcal/mol) with respect to analog 1 for Siglec-7 ($-55.89 + / - 6.53$ kcal/mol).

Overall, we found that both analogs accommodate the sialic acid residue into the binding site similarly (Figure 7A); however, in analog 1, Neu5Ac is the only part that anchors to the protein, with the rest of the molecule completely solvent exposed.

This behavior was similar to STn-Ser recognition from Siglec-15: despite low %STD effects were found for some protons of GalNAc residue, a clear preference for Neu5Ac moiety was detected.^[38] On the other hand, analog 2 contains a biphenyl moiety linked to position 9 of Neu5Ac that supports the interaction, allowing the entire ligand to get closer to the protein, resulting in a stronger affinity for Siglec-7. The flexibility of the CC' and GG' loops of Siglec-7 permits the accommodation of analog 2, overcoming the rigidity of the molecule. In detail, Phe122 and Lys135 of the GG' loop established hydrophobic interactions with the aromatic moiety, sustaining the importance of this portion of the analog 2 for the molecular interaction. Interestingly, this behavior and preference of the binding between the two analogs were opposite to those observed for the h-CD22 (Figure 7B). In this latter case, the shorter analog 1 can insert into the binding site of the protein, which selectively recognizes Neu5Ac- α -(2-6)-Gal glycosidic linkage, resulting in a complete recognition that significantly

increases the affinity to h-CD22. As for analog 2, the morphology of the protein structure hampers the canonical accommodation of the ligand that assumes a different orientation to promote the stacking interactions between the aromatic portion and the CC' loop of h-CD22.

Conclusions

We investigated the molecular recognition of structurally constrained sialyl analogs in interaction with Siglec-7. Tumor carbohydrate associated antigens (TACAs), such as the Tn and STn molecules, exhibit attractive features for diagnostic and therapeutic purposes. Our previous studies showed the syntheses of two conformationally constrained STnThr sialyl analogs and their ability to be recognized by the human CD22, inhibitory Siglec of the B cell receptor, with potential implications for developing novel therapeutics in oncology and immunology fields. Siglec-7 is another inhibitory Siglec, mainly found on NK cells, that modulates the immune response and immunosurveillance, which is, however, often subverted, thus promoting infections and tumor progression. Given its impor-

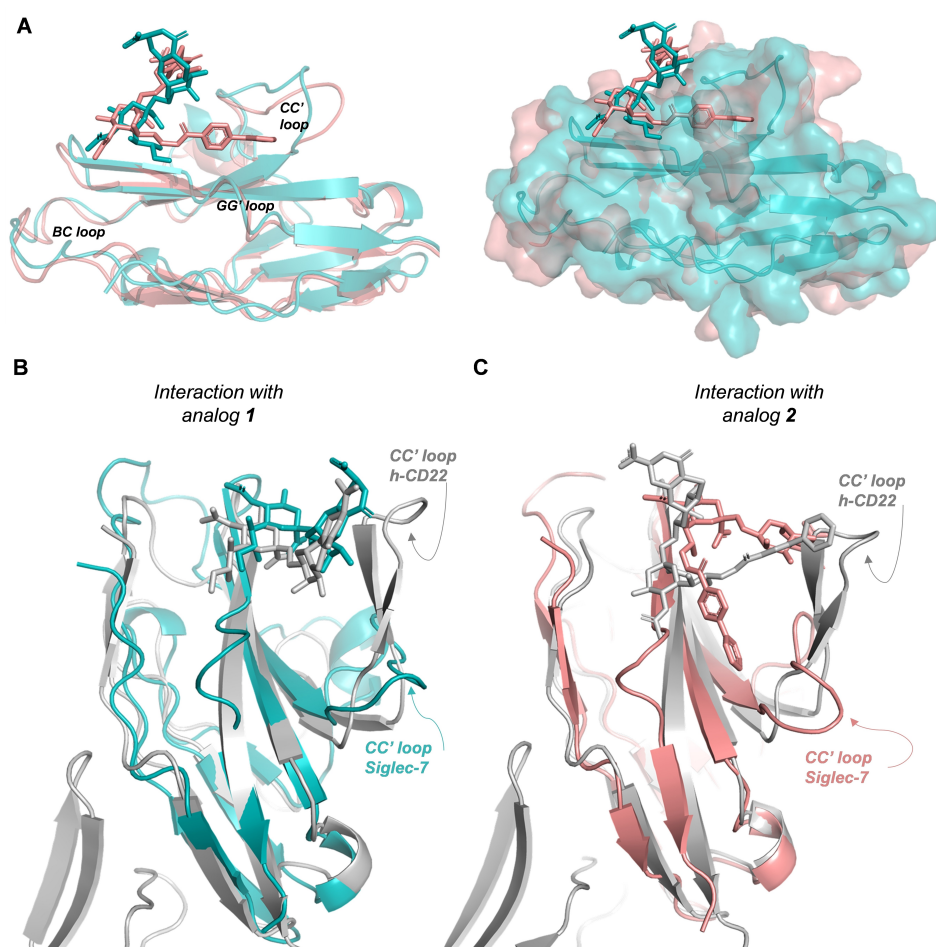


Figure 7. Comparison of the binding modes of the analogs 1 and 2 into Siglecs. A) Superimposition of the complexes of Siglec-7 with analogs 1 (cyan) and 2 (pink). B) Superimposition of the complexes of analog 1 with Siglec-7 (cyan) and h-CD22 (grey). C) Superimposition of the complexes of analog 2 with Siglec-7 (pink) and h-CD22 (grey).

tant biological role, designing new inhibitors for Siglec-7 represents an essential step for developing new therapeutic strategies. We thus decided to investigate STnThr sialyl derivatives as potential binders for Siglec-7. The molecular description of analogs **1** and **2** (Figure S1) in the interaction with Siglec-7 was provided by the combination of NOE-based techniques, like Saturation Transfer Difference and transferred-NOESY, and computational studies, including docking and molecular dynamic simulations. These findings allowed us to unveil the binding modes of the analogs into the binding site of Siglec-7, mapping the ligands epitopes, highlighting the primary contacts at the protein-ligand interface, and providing the binding affinities and the 3D models of the complexes. Our results demonstrate that an aromatic moiety extension at C9 of Neu5Ac improves the binding to Siglec-7. Moreover, we highlight the importance of the flexibility of the loops of Siglec-7, which shows a binding pocket able to accommodate highly rigid molecules, such as those containing aromatic rings. Overall, our findings provide molecular details that set the basis for the synthesis and design of novel high affinity ligands as potential modulators for the biological activity of Siglec-7 for diagnostic and therapeutic purposes.

Supporting Information

The authors have cited additional references within the Supporting Information.^[39–48]

Acknowledgements

AS, RM and SS acknowledge PNRR, Missione 4 – Componente 2 – NextGenerationEU – Partenariato Esteso INF-ACT – One Health Basic and Translational Research Actions Addressing Unmet Needs on Emerging Infectious Diseases MUR: PE00000007. This work benefited from STSM funding to CDC, OV and AS by COST Action (CA18103 INNOGLY). AS acknowledge the Ministry of Education, Universities and Research, PRIN2017 (2017XZ2ZBK, 2019–2023). CA and OV acknowledge the funding from Ministry of Education, Youth and Sports of the Czech Republic (LTC20078). This project has also received funding from the European Research Council (ERC) under the European Union's Horizon 2020 research and innovation program under grant agreement No 851356 to R.M.

Conflict of Interests

The authors declare no conflict of interest.

Data Availability Statement

The data that support the findings of this study are available from the corresponding author upon reasonable request.

Keywords: computational studies · molecular binding · sialo-derivatives · siglecs · NMR spectroscopy

- [1] S. Duan, J. C. Paulson, *Annu. Rev. Immunol.* **2020**, *38*, 365–395.
- [2] T. Angata, A. Varki, *Mol. Aspects Med.* **2023**, *90*, 101117.
- [3] C. Di Carluccio, R. E. Forgione, A. Molinaro, P. R. Crocker, R. Marchetti, A. Sillipo in *Exploring the fascinating world of sialoglycans in the interplay with Siglecs* **2020**, pp. 31–55.
- [4] S. Pillai, I. A. Netravali, A. Cariappa, H. Mattoo, *Annu. Rev. Immunol.* **2012**, *30*, 357–392.
- [5] P. R. Crocker, J. C. Paulson, A. Varki, *Nat. Rev. Immunol.* **2007**, *7*, 255–266.
- [6] L.-Y. Chang, S.-Y. Liang, S.-C. Lu, H. C. Tseng, H.-Y. Tsai, C.-J. Tang, M. Sugata, Y.-J. Chen, Y.-J. Chen, S.-J. Wu, *Front. Immunol.* **2022**, *13*.
- [7] C. Jandus, K. F. Boligan, O. Chijioko, H. Liu, M. Dahlhaus, T. Démoulin, C. Schneider, M. Wehrli, R. E. Hunger, G. M. Baerlocher, *The Journal of clinical investigation* **2014**, *124*, 1810–1820.
- [8] M. S. Alphey, H. Attrill, P. R. Crocker, D. M. van Aalten, *J. Biol. Chem.* **2003**, *278*, 3372–3377.
- [9] L. Tao, S. Wang, L. Yang, L. Jiang, J. Li, X. Wang, *Clin. Exp. Immunol.* **2020**, *201* (2), 161–170.
- [10] J. E. Hudak, S. M. Canham, C. R. Bertozzi, *Nat. Chem. Biol.* **2014**, *10* (1), 69–75.
- [11] E. Rodriguez, K. Boelaars, K. Brown, R. Eveline Li, L. Kruijssen, S. C. Bruijns, T. van Ee, S. T. Schetters, M. H. Crommentuijn, J. C. van der Horst, *Nat. Commun.* **2021**, *12*, 1270.
- [12] A. Ito, K. Handa, D. A. Withers, M. Satoh, S.-i. Hakomori, *FEBS Lett.* **2001**, *504*, 82–86.
- [13] Y. Kawasaki, A. Ito, D. A. Withers, T. Taima, N. Kakoi, S. Saito, Y. Arai, *Glycobiology* **2010**, *20*, 1373–1379.
- [14] B. A. Smith, C. R. Bertozzi, *Nat. Rev. Drug Discovery* **2021**, *20*, 217–243.
- [15] C. Di Carluccio, E. Crisman, Y. Manabe, R. E. Forgione, A. Lacetera, J. Amato, B. Pagano, A. Randazzo, A. Zampella, R. Lanzetta, *ChemBioChem* **2020**, *21*, 129–140.
- [16] C. Büll, R. Nason, L. Sun, J. Van Coillie, D. Madriz Sørensen, S. J. Moons, Z. Yang, S. Arbitman, S. M. Fernandes, S. Furukawa, R. McBride, C. M. Nycholat, G. J. Adema, J. C. Paulson, R. L. Schnaar, T. J. Boltje, H. Clausen, Y. Narimatsu, *Proc. Natl. Acad. Sci. USA* **2021**, *118*, 17, e2026102118.
- [17] T. Iwasawa, P. Zhang, Y. Ohkawa, H. Momota, T. Wakabayashi, Y. Ohmi, R. H. Bhuiyan, K. Furukawa, K. Furukawa, *Int. J. Oncol.* **2018**, *52*, 1255–1266.
- [18] C. P. Swaminathan, N. Wais, V. V. Vyasa, C. A. Velikovskiy, A. Moretta, L. Moretta, R. Biassoni, R. A. Mariuzza, N. Dimasi, *ChemBioChem* **2004**, *5*, 1571–1575.
- [19] H. Attrill, A. Imamura, R. S. Sharma, M. Kiso, P. R. Crocker, D. M. Van Aalten, *J. Biol. Chem.* **2006**, *281*, 32774–32783.
- [20] R. E. Forgione, F. F. Nieto, C. Di Carluccio, F. Milanese, M. Fruscella, F. Papi, C. Nativi, A. Molinaro, P. Palladino, S. Scarano, *ChemBioChem* **2022**, *23*, e202200076.
- [21] A. Ardá, R. Bosco, J. Sastre, F. J. Cañada, S. André, H.-J. Gabius, B. Richichi, J. Jiménez-Barbero, C. Nativi, *Eur. J. Org. Chem.* **2015**, 6823–6831.
- [22] S. Santarsia, A. S. Grosso, F. Trovão, J. Jiménez-Barbero, A. L. Carvalho, C. Nativi, F. Marcelo, *ChemMedChem* **2018**, *13* (19), 2030–2036.
- [23] C. D. Rillaha, E. Schwartz, C. Rademacher, R. McBride, J. Rangarajan, V. V. Fokin, J. C. Paulson, *ACS Chem. Biol.* **2013**, *8* (7), 1417–22.
- [24] C. D. Rillaha, E. Schwartz, R. McBride, V. V. Fokin, J. C. Paulson, *Angew. Chem. Int. Ed. Engl.* **2012**, *51* (44), 11014–8.
- [25] M. P. Lenza, U. Atxabal, C. Nycholat, I. Oyenarte, A. Franconetti, J. I. Quintana, S. Delgado, R. Núñez-Franco, C. T. Garnica Marroquín, H. Coelho, L. Unione, G. Jiménez-Oses, F. Marcelo, M. Schubert, J. C. Paulson, J. Jiménez-Barbero, J. Ereño-Orbea, *JACS* **2022**, *3* (1), 204–215.
- [26] F. Papi, A. Pàris, P. Lafite, R. Daniellou, C. Nativi, *Org. Biomol. Chem.* **2020**, *18*, 7366–7372.
- [27] C. Nativi, F. Papi, S. Roelens, *Chem. Commun.* **2019**, *55*, 7729–7736.
- [28] R. Marchetti, S. Perez, A. Arda, A. Imberty, J. Jimenez-Barbero, A. Sillipo, A. Molinaro, *ChemistryOpen* **2016**, *5*, 274–296.
- [29] J. Angulo, P. M. Nieto, *Eur. Biophys. J.* **2011**, *40*, 1357–1369.
- [30] C. Di Carluccio, M. C. Forgione, S. Martini, F. Berti, A. Molinaro, R. Marchetti, A. Sillipo, *Carbohydr. Res.* **2021**, *503*, 108313.
- [31] C. Oliveira Soares, A. S. Grosso, J. Ereño-Orbea, H. Coelho, F. Marcelo, *Front. Mol. Biosci.* **2021**, *8*, 727847.
- [32] R. E. Forgione, C. Di Carluccio, J. Guzmán-Caldentey, R. Gaglione, F. Battista, F. Chiodo, Y. Manabe, A. Arciello, P. Del Vecchio, K. Fukase, A.

- Molinaro, S. Martín-Santamaría, P. R. Crocker, R. Marchetti, A. Silipo. *iScience* **2020**, *23*, 101231.
- [33] R. A. Friesner, J. L. Banks, R. B. Murphy, T. A. Halgren, J. J. Klicic, D. T. Mainz, M. P. Repasky, E. H. Knoll, M. Shelley, J. K. Perry, D. E. Shaw, P. Francis, P. S. Shenkin, *J. Med. Chem.* **2004**, *47* (7), 1739–1749.
- [34] K. J. Bowers, E. Chow, H. Xu, R. O. Dror, M. P. Eastwood, B. A. Gregersen, J. L. Klepeis, I. Kolossvary, M. A. Moraes, F. D. Sacerdoti, J. K. Salmon, Y. Shan, D. E. Shaw, *Desmond* (Schrodinger release 2018–1). Proceedings of the ACM/IEEE Conference on Supercomputing (SC06), Tampa (Florida) **2006**, 43.
- [35] C. D. Berweger, W. F. van Gunsteren, F. Müller-Plathe, *Chem. Phys. Lett.* **1995**, *232* (5–6), 429–436.
- [36] J. Angulo, P. M. Enriquez-Navas, P. M. Nieto, *Chem. Eur. J.* **2010**, *16*, 7803–7812.
- [37] J. P. Ribeiro, S. André, F. Javier Cañada, H. J. Gabius, A. P. Butera, R. J. Alves, J. Jiménez-Barbero, *ChemMedChem* **2010**, *5*, 415–419.
- [38] M. P. Lenza, L. Egia-Mendikute, A. Antoñana-Vildosola, C. O. Soares, H. Coelho, F. Corzana, A. Bosch, P. Manisha, J. Imanol Quintana, I. Oyentearte, L. Unione, M. Jesús Moure, M. Azkargorta, U. Atxabal, K. Sobczak, F. Elortza, J. D. Sutherland, R. Barrio, F. Marcelo, J. Jiménez-Barbero, A. Palazon, J. Ereño-Orbea, *Nat. Commun.* **2023**, *14*, 3496.
- [39] I. Speciale, A. Notaro, P. Garcia-Vello, F. Di Lorenzo, S. Armiento, A. Molinaro, R. Marchetti, A. Silipo, C. De Castro, *Carbohydr. Polym.* **2022**, *277*, 118885.
- [40] R. Marchetti, R. E. Forgione, F. Nieto Fabregat, C. Di Carluccio, A. Molinaro, A. Silipo, *Current Opinion in Structural Biology* **2020**, *68*, 74–83.
- [41] P. J. Reeves, N. Callewaert, R. Contreras, H. G. Khorana, *Proc. Natl. Acad. Sci. USA* **2002**, *15* (99, 21), 13419–24.
- [42] J. Bláha, P. Pachl, P. Novák, O. Vanek, *Protein Expression Purif.* **2015**, *109*, 7–13.
- [43] O. Vaněk, P. Celadova, O. Škořepa, J. Bláha, B. Kalousková, A. Dvorská, E. Poláková, H. Pucholtová, D. Kavan, P. Pompach, K. Hofbauerová, V. J. Kopecký, A. Mesci, S. Voigt, J. R. Carlyle, *Sci. Rep.* **2019**, *9* (1), 17836.
- [44] K. Roos, C. Wu, W. Damm, M. Reboul, J. M. Stevenson, C. Lu, M. K. Dahlgren, S. Mondal, W. Chen, L. Wang, R. Abel, R. A. Friesner, E. D. Harder, *J. Chem. Theory Comput.* **2019**, *15* (3), 1863–1874.
- [45] S. Gary, K. Kremer, *Molecular dynamics simulation for polymers in the presence of a heat bath. Phys. Rev. A.* **1986**, *33*, 3628.
- [46] C. Predescu, A. K. Lerer, R. A. Lippert, B. Towles, J. P. Grossman, R. M. Dirks, D. E. Shaw, *J. Chem. Phys.* **2020**, *152* (8), 084113.
- [47] M. P. Jacobson, D. L. Pincus, C. S. Rapp, T. J. F. Day, B. Honig, D. E. Shaw, R. A. Friesner, *Proteins* **2004**, *55*, 351–367.
- [48] J. Li, R. Abel, K. Zhu, Y. Cao, S. Zhao, R. A. Friesner, *Proteins* **2011**, *79*, 2794–2812.

Manuscript received: June 30, 2023
 Revised manuscript received: August 11, 2023
 Accepted manuscript online: August 11, 2023
 Version of record online: September 11, 2023